Asian Journal of Chemistry; Vol. 32, No. 12 (2020), 3209-3218

ASIAN JOURNAL OF CHEMISTRY

https://doi.org/10.14233/ajchem.2020.22956

Design and Synthesis of 2-Mercapto Benzoxazole coupled Benzyl Triazoles as Anti-inflammatory Agents Targeting COX-2 Enzyme

K. Praveen Kumar[1], Y. Prashanthi[2,*], G. Rambabu[3], Md. Ataur Rahman[4] and J.S. Yadav[1,5,*]

[1]Fluoro Agro Chemicals, C.S.I.R.-Indian Institute of Chemical Technology, Tarnaka, Hyderabad-500007, India
[2]Department of Chemistry, Mahatma Gandhi University, Nalgonda-508001, India
[3]Department of Chemistry, School of Technology, GITAM, Hyderabad-502329, India
[4]Department of Chemistry and Chemical Biology, Harvard University, Cambridge, Massachusetts 02138, U.S.A.
[5]School of Science, Indrashil University, Kadi, Mehsana, Gujarat-382740, India

*Corresponding authors: E-mail: puttaprashanthi@gmail.com; yadavfna@gmail.com

Received: 20 August 2020; *Accepted*: 5 November 2020; *Published online*: 7 December 2020; AJC-20163

In this study, we report the design, synthesis and the biological evaluation of 19 analogues of 2-mercapto benzoxazole coupled benzyl triazoles (BOTs) based on analysis of the binding site and literature of chemical space. These BOTs were evaluated both *in vitro* and *in vivo* for their anti-inflammatory activity. Eleven compounds showed less than 10 µM *in vitro* COX-2 enzyme activities. The most potent analogue among the BOT analogues were BOT15, BOT3 and BOT19 with IC_{50} 3.40 µM, 4.50 µM and 4.57 µM respectively against COX-2. The *in vivo* anti-inflammatory activity of two BOTs has significantly higher than that of standard drug, ibuprofen. 2-Mercapto benzoxazole coupled benzyl triazoles (BOTs) were also tested for their antioxidant capacity and proved to be an as active scavenger, better than ascorbic acid.

Keywords: 2-Mercapto benzoxazole, Benzyl Triazoles, Anti-inflammatory, Anti-oxidants, Cyclooxgenase-1, Cyclooxygenase-2.

INTRODUCTION

Every 3 out of 5 folks expire because of chronic inflammatory ailments and world health organization describes inflammatory disorders as the paramount risk to human wellbeing [1]. Cyclooxygenase (COX) is the enzyme that contributes to inflammation and its inhibitors are usually used to lessen the agony. Non-steroidal anti-inflammatory drugs (NSAIDs) are generally used for the inhibition of COX-1 and COX-2 [2]. Due to the selectivity issues, COX-2 is widely studied target when compared to COX-1. Out of 2 isoforms, COX-1 is expressed in many tissues, but COX-2 typically is absent [3]. Celecoxib and rofecoxib even with a high amount of selectivity towards COX-2 were withdrawn from the market due to severe toxicity issues [4]. These inhibitors were also used in many diseases like cancer, autoimmune diseases, obesity, metabolic syndrome, neurodegenerative diseases, atherosclerosis and arthritis and there is a need to increase the spectrum of cyclooxygenase inhibitors [5].

In this context, a plethora of research was carried out throughout the world and different chemical moieties were explored and out of which pyrazole [6,7], indole [8,9], pyridine [10,11], oxazole [12,13], pyrrole [14,15] played a major role as anti-inflammatory agents. In some studies, 1,2-benzothiazole-3(2*H*)-one-1,1-dioxide analogous comprising both aryl hydrazones and five-membered heterocyclic rings were assessed for their *in vitro* COX-1/COX-2 inhibitory activity [16]. Different pyridazinone derivatives in combination with aryl or pyridyl rings linked *via* an ethenyl piece were synthe-sized and proved to be effective against cyclooxygenases both in *in vitro* and *in vivo* studies [17].

A series of novel indazole derivatives which were proved to be active and selective to COX-2 were radiolabeled (^{18}F) and the tracer was evaluated *in vivo* in a neuroinflammation model [18]. Molecular modelling has played a major role in filling the gaps in experimental validity and contributed to the evolution of many active moieties [19]. Using the latest trends in the designing and discovery, our group previously synthesized

2-(((5-aryl-1,2,4-oxadiazol-3-yl)methyl)thio)benzo[*d*]oxazoles and 2-mercapto benzothiazole linked 1,2,4-oxadiazoles and proved that these moieties were active in *in vitro* and *in vivo* studies [20,21]. In present work, we have designed a new class of 2-mercapto benzoxazole coupled benzyl triazoles (BOT) based on the extensive analysis of the binding pocket of COX-1 and COX-2, our previous experience on designing of novel COX-2 inhibitors and known literature Fig. 1 [22-24]. All the designed molecules were synthesized and tested using *in vitro*, *in vivo* studies and confirmed as new and efficient anti-inflammatory agents.

EXPERIMENTAL

All the chemicals were purchased from Alfa Aeser (Alfa Aesar, Johnson Matthey Co., USA), Sigma-Aldrich (USA) and Spectrochem Pvt. Ltd. (India). The progress of the reaction was monitored by TLC. Silica gel-G plates (Merck) were used for TLC analysis with a mixture of petroleum ether and ethyl acetate as the eluent, visualization on TLC was achieved by UV light. ^{1}H NMR spectra were recorded on Avance (300 MHz); Bruker, Fallanden, Switzerland instruments. ESI spectra were recorded on Micro mass, Quattro LC using ESI+ software with a capillary voltage of 3.98 kV and ESI mode positive ion trap detector. IR spectra were recorded on an FT-IR spectrometer (Shimadzu FT-IR 8300 spectrophotometer). The melting point was meas-ured in open capillary tubes and results were uncorrected. All the synthesized compounds were characterized by their physical and spectral data.

2-(Prop-2-yn-1-ylthio)benzo[*d*]oxazole (2): Propargyl bromide (80%) in toluene (4.90 mL, 39.72 mmol) was added to a stirred solution of benzo[*d*]oxazole-2-thiol **(1)** (5.00 g, 33.1 mmol) and K_2CO_3 (6.85 g, 49.60 mmol) in DMF (50 mL) and allowed the reaction mixture to stir at room temperature

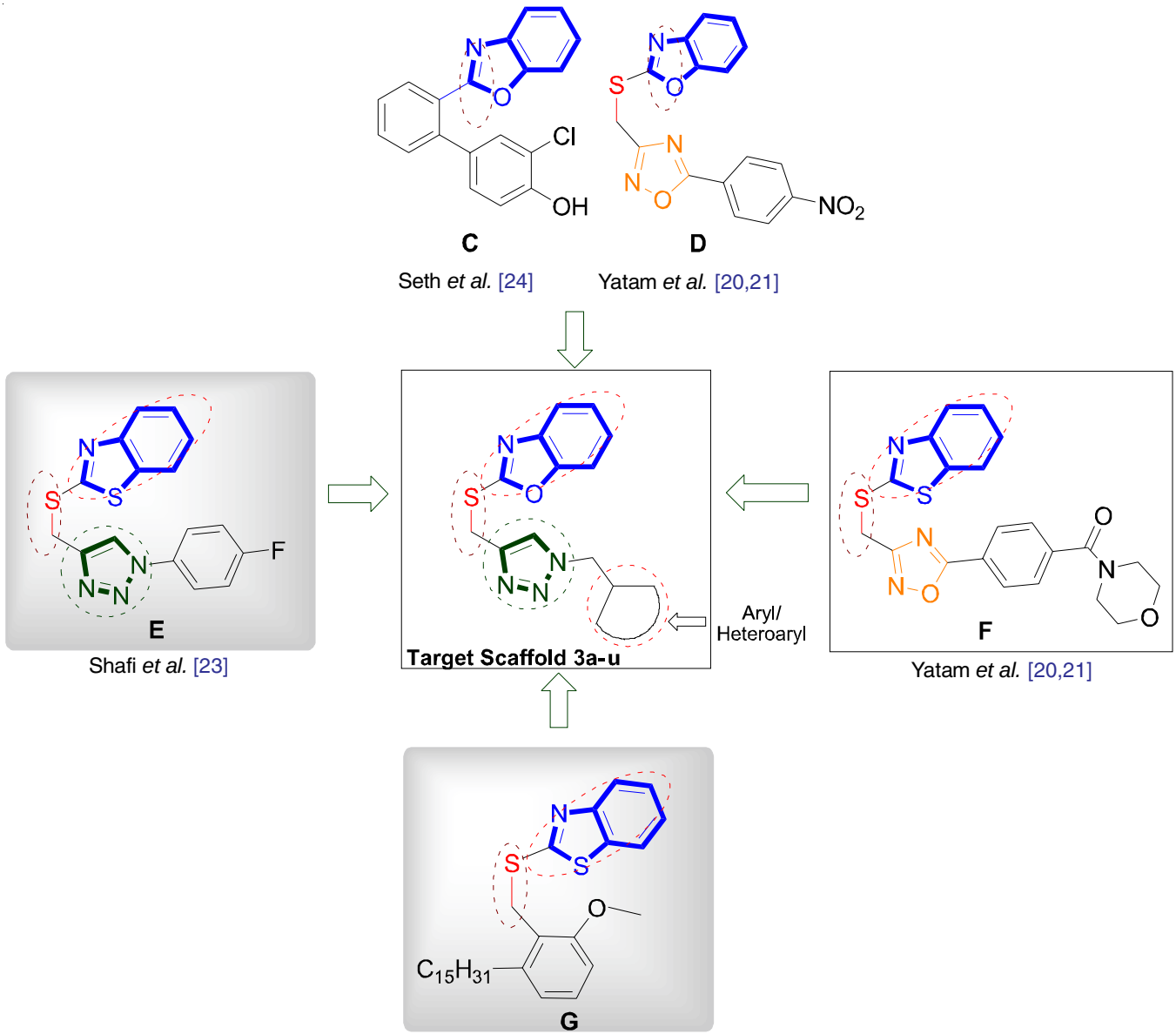

Fig. 1. Design of scaffold for selective COX-2 inhibition through the scaffold-hopping approach

for 1 h under nitrogen. Reaction was monitored by TLC (R_f = 0.55, pet. ether:EtOAc = 7:3), after completion of reaction, water (200 mL) was added to the reaction mixture was extracted with EtOAc (150 mL) and the organic layer was washed with water (3 × 200 mL) followed by brine solution (200 mL). The organic layer was dried over anhydrous Na_2SO_4, filtered and concentrated in vacuo and the residue was purified by column chromatography over silica gel (100-200 mesh) with eluent 10% EtOAc in pet ether to afford 2-(prop-2-yn-1-ylthio)benzo-[*d*]oxazole (2) (5.63 g, 29.79 mmol, 90%) as a light brown-orange gummy solid. ^{1}H NMR (400 MHz, $CDCl_3$) δ: 7.63-7.61 (m, 1H), 7.45-7.43 (m, 1H), 7.30-7.22 (m, 2H), 4.07 (d, *J* = 2.40 Hz, 2H), 2.30 (t, *J* = 2.8 Hz, 1H). ^{13}C NMR (100 MHz, $CDCl_3$) δ: 163.05, 152.04, 141.76, 124.46, 124.21, 118.70, 110.04, 77.93, 72.49, 20.72.

General procedure for the synthesis of 2-mercapto benzoxazole coupled benzyl triazoles (BOTs) (1-19): Sodium ascorbate (1.57 mmol) was added to a green coloured suspension of $Cu(OAc)_2{\cdot}H_2O$ (0.105 mmol) and 1,10-phenanthroline monohydrate (0.105 mmol) in 4:1 EtOH and H_2O (8 mL: 2 mL) and stirred the reaction mixture for 5 min at room temperature, then added 2-(prop-2-yn-1-ylthio)benzo[*d*]thiazole (**2**) (1.05 mmol), sodium azide (1.26 mmol) and benzyl bromide derivative (1.15 mmol) and the resulting orange coloured suspension was stirred at room temperature for 18 h. After 18 h, diluted the reaction mixture with water (30 mL) and extracted with EtOAc (50 mL). The organic layer was washed with water (30 mL) followed by brine (30 mL), the organic layer was dried over anhydrous Na_2SO_4, filtered and concentrated in vacuo and the residue was purified by column chromatography over silica gel (100-200 mesh) with eluent 50% to 70 % EtOAc in pet ether followed by recrystallization with diethyl ether to yield compound.

2-(((1-(Naphthalen-1-ylmethyl)-1*H*-1,2,3-triazol-4-yl)methyl)thio)benzo[*d*]oxazole (BOT-1): Yield: 75%; off-white solid; m.p.: 65-67 ºC; IR (KBr, ν_{max}, cm^{-1}): 1496, 1448, 1234, 1220, 1128, 791; ^{1}H NMR (400 MHz, $CDCl_3$) δ: 7.91-7.85 (m, 3H), 7.50-7.35 (m, 7H), 7.29-7.21 (m, 2H), 5.92 (s, 2H), 4.54 (s, 2H). ^{13}C NMR (100 MHz, $CDCl_3$) δ: 163.58, 151.43, 143.08, 141.19, 133.37, 130.57, 129.56, 129.17, 128.43, 127.30, 126.76, 125.90, 124.84, 123.81, 123.50, 122.44, 122.24, 117.89, 109.45, 51.84, 26.31. LC-MS (ESI+APCI): *m/z* = 373 $[M+H]^+$.

2-(((1-(Naphthalen-2-ylmethyl)-1*H*-1,2,3-triazol-4-yl)methyl)thio)benzo[*d*]oxazole (BOT-2): Yield: 75%; off-white solid; m.p.: 79-81 ºC; IR (KBr, ν_{max}, cm^{-1}): 1504, 1451, 1236, 1215, 1126, 748; ^{1}H NMR (400 MHz, $CDCl_3$) δ: 7.83-7.75 (m, 3H), 7.69 (s, 1H), 7.61 (s, 1H), 7.52-7.47 (m, 3H), 7.40-7.38 (m, 1H), 7.30-7.19 (m, 3H), 5.63 (s, 2H), 4.60 (s, 2H). ^{13}C NMR (100 MHz, $CDCl_3$) δ: 164.18, 152.00, 143.94, 141.75, 133.17, 131.77, 129.16, 127.95, 127.79, 127.38, 126.74, 125.25, 124.33, 124.03, 123.01, 118.41, 109.99, 54.40, 26.86. LC-MS (ESI+APCI): *m/z* = 373 $[M+H]^+$.

2-(((1-(2-Methylbenzyl)-1*H*-1,2,3-triazol-4-yl)methyl)-thio)benzo[*d*]oxazole (BOT-3): Yield: 70%; off-white solid; m.p.: 55-57 ºC; IR (KBr, ν_{max}, cm^{-1}): 1498, 1451, 1221, 1131, 756; ^{1}H NMR (400 MHz, $CDCl_3$) δ: 7.55-7.52 (m, 1H), 7.47 (s, 1H), 7.39 (dd, *J* = 7.6 Hz, 1.6 Hz, 1H), 7.29-7.21 (m, 3H), 7.17-7.14 (m, 2H), 7.08-7.06 (m, 1H), 5.46 (s, 2H), 4.57 (s, 2H), 2.19 (s, 3H). ^{13}C NMR (100 MHz, $CDCl_3$) δ: 164.14, 151.98, 143.53, 141.76, 136.82, 132.33, 131.02, 129.31, 129.14, 126.64, 124.33, 124.05, 122.77, 118.41, 109.98, 52.38, 26.89, 18.90. LC-MS (ESI+APCI): *m/z* = 337 $[M+H]^+$.

2-(((1-(4-Methylbenzyl)-1*H*-1,2,3-triazol-4-yl)methyl)-thio)benzo[*d*]oxazole (BOT-4): Yield: 85%; off-white solid; m.p.: 58-60 ºC; IR (KBr, ν_{max}, cm^{-1}): 1506, 1449, 1233, 1131, 760; ^{1}H NMR (400 MHz, $CDCl_3$) δ: 7.56-7.55 (m, 2H), 7.41-7.39 (m, 1H), 7.30-7.21 (m, 2H), 7.11 (s, 4H), 5.42 (s, 2H), 4.58 (s, 2H), 2.32 (s, 3H). ^{13}C NMR (100 MHz, $CDCl_3$) δ: 164.23, 152.01, 143.70, 141.79, 138.68, 131.41, 129.76, 128.07, 124.32, 124.03, 122.75, 118.42, 110.00, 54.00, 26.88, 21.16. LC-MS (ESI+APCI): *m/z* = 337 $[M+H]^+$.

2-(((1-(4-Isopropylbenzyl)-1*H*-1,2,3-triazol-4-yl)-methyl)thio)benzo[d]oxazole (BOT-5): Yield: 78%; off-white solid; m.p.: 53-55 ºC; IR (KBr, ν_{max}, cm^{-1}): 1498, 1449, 1230, 1127, 746; ^{1}H-NMR (400 MHz, $CDCl_3$) δ: 7.59-7.55 (m, 2H), 7.42-7.40 (m, 1H), 7.29-7.13 (m, 6H), 5.43 (s, 2H), 4.59 (s, 2H), 2.91-2.84 (m, 1H), 1.22 (d, *J* = 7.2 Hz, 6H). ^{13}C NMR (100 MHz, $CDCl_3$) δ: 164.25, 152.01, 149.60, 143.68, 141.79, 131.75, 128.12, 127.16, 124.33, 124.04, 122.83, 118.42, 110.01, 53.99, 33.84, 26.89, 23.89. LC-MS (ESI+APCI): *m/z* = 365 $[M + H]^+$.

2-(((1-(4-(*tert*-Butyl)benzyl)-1*H*-1,2,3-triazol-4-yl)-methyl)thio)benzo[d]oxazole (BOT-6): Yield: 80%; off-white solid; m.p.: 56-58 ºC; IR (KBr, ν_{max}, cm^{-1}): 1502, 1450, 1216, 1132, 736; ^{1}H NMR (400 MHz, $CDCl_3$) δ: 7.59 (s, 1H), 7.57 (d, *J* = 7.2 Hz, 1H), 7.41 (d, *J* = 7.6 Hz, 1H), 7.34 (d, *J* = 8.0 Hz, 2H), 7.29–7.22 (m, 2H), 7.15 (d, *J* = 8.0 Hz, 2H), 5.44 (s, 2H), 4.59 (s, 2H), 1.29 (s, 9H). ^{13}C NMR (100 MHz, $CDCl_3$) δ: 164.25, 152.02, 151.89, 143.68, 141.79, 131.40, 127.83, 126.03, 124.34, 124.04, 122.86, 118.42, 110.01, 53.90, 34.64, 31.26, 26.88. LC-MS (ESI+APCI): *m/z* = 379 $[M+H]^+$.

2-(((1-(4-Methoxybenzyl)-1*H*-1,2,3-triazol-4-yl)methyl)-thio)benzo[*d*]oxazole (BOT-7): Yield: 77%; off-white solid; m.p.: 70-72 ºC; IR (KBr, ν_{max}, cm^{-1}): 1610, 1502, 1450, 1243, 1129, 734; ^{1}H-NMR (400 MHz, $CDCl_3$) δ: 7.57-7.56 (m, 2H), 7.40 (d, *J* = 7.6 Hz, 1H), 7.29-7.21 (m. 2H), 7.16 (d, *J* = 8.4 Hz, 2H), 6.83 (d, *J* = 8.8 Hz, 2H), 5.39 (s, 2H), 4.58 (s, 2H), 3.77 (s, 3H). ^{13}C NMR (100 MHz, $CDCl_3$) δ: 164.21, 159.89, 151.99, 143.65, 141.76, 129.61, 126.38, 124.33, 124.04, 122.67, 118.41, 114.44, 110.0, 55.32, 53.74, 26.85. LC-MS (ESI+APCI): m/z = 353 $[M+H]^+$.

2-(((1-(2-Fluorobenzyl)-1*H*-1,2,3-triazol-4-yl)methyl)-thio)benzo[*d*]oxazole (BOT-8): Yield: 72%; off-white solid; m.p.: 67-69 ºC; IR (KBr, ν_{max}, cm^{-1}): 1497, 1240, 1133, 1098, 762; ^{1}H NMR (400 MHz, $CDCl_3$) δ: 7.71 (s, 1H), 7.59-7.57 (m, 1H), 7.42-7.40 (m, 1H), 7.34-7.19 (m, 4H), 7.10-7.04 (m, 2H), 5.52 (s, 2H), 4.60 (s, 2H). ^{13}C NMR (100 MHz, $CDCl_3$) δ: 164.17, 161.71, 159.24, 152.01, 143.82, 141.76, 130.96, 130.88, 130.50, 130.47, 124.84, 124.80, 124.35, 124.05, 123.14, 123.13, 121.84, 121.70, 118.43, 115.91, 115.70, 110.00, 47.77, 26.81. LC-MS (ESI+APCI): *m/z* = 341 $[M+H]^+$.

2-(((1-(3-Fluorobenzyl)-1*H*-1,2,3-triazol-4-yl)methyl)-thio)benzo[*d*]oxazole (BOT-9): Yield: 80%; off-white solid; m.p.: 69-71 ºC; IR (KBr, ν_{max}, cm^{-1}):1495, 1247, 1135, 744;

^{1}H-NMR (400 MHz, $CDCl_3$) δ: 7.65 (s, 1H), 7.57 (dd, *J* = 8.0 Hz, 1.2 Hz, 1H), 7.42 (dd, *J* = 7.6 Hz, 0.4 Hz, 1H), 7.30-7.22 (m, 3H), 7.03-6.97 (m, 2H), 6.93-6.90 (m, 1H), 5.46 (s, 2H), 4.60 (s, 2H). ^{13}C NMR (100 MHz, $CDCl_3$) δ: 164.18, 161.72, 152.02, 144.13, 141.73, 136.86, 136.79, 130.81, 130.72, 124.37, 124.09, 123.49, 123.46, 122.99, 118.41, 115.89, 115.68, 115.06, 114.84, 110.02, 53.51, 26.79. LC-MS (ESI+APCI): *m/z* = 341 $[M+H]^+$.

2-(((1-(4-Fluorobenzyl)-1*H*-1,2,3-triazol-4-yl)methyl)thio)benzo[*d*]oxazole (BOT-10): Yield: 75%; off-white solid; m.p.: 70-72 ºC; IR (KBr, ν_{max}, cm^{-1}): 1506, 1452, 1220, 1130, 743; ^{1}H NMR (400 MHz, $CDCl_3$) δ: 7.60 (s, 1H), 7.57-7.55 (m, 1H), 7.41-7.39 (m, 1H), 7.30-7.18 (m, 4H), 7.01-6.96 (m, 2H), 5.43 (s, 2H), 4.59 (s, 2H). ^{13}C NMR (100 MHz, $CDCl_3$) δ: 164.14, 164.03, 161.57, 151.99, 143.97, 141.73, 130.35, 130.32, 129.93, 129.84, 124.37, 124.10, 122.82, 118.39, 116.19, 115.97, 110.01, 53.40, 26.82. LC-MS (ESI+APCI): *m/z* = 341 $[M+H]^+$.

2-(((1-(2,4-Difluorobenzyl)-1*H*-1,2,3-triazol-4-yl)methyl)thio)benzo[*d*]oxazole (BOT-11): Yield: 75%; off-white solid; m.p.: 77-79 ºC; IR (KBr, ν_{max}, cm^{-1}): 1506, 1273, 1141, 739; ^{1}H NMR (400 MHz, $CDCl_3$) δ: 7.69 (s, 1H), 7.59-7.57 (m, 1H), 7.43-7.41 (m, 1H), 7.31-7.19 (m, 3H), 6.85-6.79 (m, 2H), 5.48 (s, 2H), 4.60 (s, 2H). ^{13}C NMR (100 MHz, $CDCl_3$) δ: 164.60, 164.48, 164.14, 162.10, 161.98, 161.96, 161.84, 159.47, 159.35, 152.02, 144, 141.76, 131.62,131.58, 131.53, 131.48, 124.36, 124.08, 122.99, 118.41, 118.0, 117.96, 117.86, 117.82, 112.26, 112.22, 112.04, 112.01, 110.0, 104.61, 104.36, 104.11, 47.19, 47.16, 26.79. LC-MS (ESI+APCI): *m/z* = 359 $[M+H]^+$.

2-(((1-(3,4-Difluorobenzyl)-1*H*-1,2,3-triazol-4-yl)methyl)thio)benzo[*d*]oxazole (BOT-12): Yield: 75%; off-white solid; m.p.: 71-73 ºC; IR (KBr, ν_{max}, cm^{-1}): 1510, 1213, 1127, 739; ^{1}H NMR (400 MHz, $CDCl_3$) δ: 7.65 (s, 1H), 7.58-7.55 (m, 1H), 7.42-7.40 (m, 1H), 7.30-7.22 (m, 2H), 7.12-7.02 (m, 2H), 6.96-6.93 (m, 1H), 5.42 (s, 2H), 4.60 (s, 2H). ^{13}C NMR (100 MHz, $CDCl_3$) δ: 164.09, 152.02, 151.78, 151.66, 149.30, 149.18, 144.27, 141.72, 131.51, 131.46, 131.42, 124.38, 124.12, 122.88, 118.38, 118.06, 117.88, 117.22, 117.04, 110.00, 52.99, 26.78. LC-MS (ESI+APCI): *m/z* = 359 $[M+H]^+$.

2-(((1-(2-Chlorobenzyl)-1*H*-1,2,3-triazol-4-yl)methyl)thio)benzo[*d*]oxazole (BOT-13): Yield: 70%; off-white solid; m.p.: 65-67 ºC; IR (KBr, ν_{max}, cm^{-1}): 1498, 1239, 1130, 759; ^{1}H NMR (400 MHz, $CDCl_3$) δ: 7.72 (s, 1H), 7.57 (d, *J* = 7.6 Hz, 1H), 7.42-7.37 (m, 2H), 7.30-7.18 (m, 4H), 7.11 (d, *J* = 7.6 Hz, 1H), 5.60 (s, 2H), 4.61 (s, 2H). ^{13}C NMR (100 MHz, $CDCl_3$) δ: 164.16, 152.01, 143.74, 141.77, 133.42, 132.31, 130.24, 129.90, 127.58, 124.35, 124.06, 123.33, 118.43, 110.00, 51.47, 26.84. LC-MS (ESI+APCI): *m/z* = 357 $[M+H]^+$.

2-(((1-(3-Chlorobenzyl)-1*H*-1,2,3-triazol-4-yl)methyl)thio)benzo[*d*]oxazole (BOT-14): Yield: 73%; off-white solid; m.p.: 72-74 ºC; IR (KBr, ν_{max}, cm^{-1}): 1498, 1214, 1137, 736; ^{1}H NMR (400 MHz, $CDCl_3$) δ: 7.63 (s, 1H), 7.58-7.56 (m, 1H), 7.42-7.40 (m, 1H), 7.30-7.21 (m, 5H), 7.07 (d, *J* = 7.6 Hz, 1H), 5.44 (s, 2H), 4.60 (s, 2H). ^{13}C NMR (100 MHz, $CDCl_3$) δ: 164.16, 152.03, 144.16, 141.75, 136.39, 134.98, 130.40, 128.98, 128.05, 126.01, 124.37, 124.09, 122.97, 118.43, 110.02, 53.46, 26.79. LC-MS (ESI+APCI): *m/z* = 357 $[M+H]^+$.

2-(((1-(3,4-Dichlorobenzyl)-1*H*-1,2,3-triazol-4-yl)methyl)thio)benzo[*d*]oxazole (BOT-15): Yield: 77%; off-white solid; m.p.: 75-77 ºC; IR (KBr, ν_{max}, cm^{-1}): 1501, 1448, 1212, 1130, 743; ^{1}H NMR (400 MHz, DMSO-d_6) δ: 7.65 (s, 1H), 7.58-7.56 (m, 1H), 7.43-7.41 (m, 1H), 7.38-7.35 (m, 1H), 7.32-7.24 (m, 3H), 7.02 (dd, *J* = 8.0 Hz, 2.0 Hz, 1H), 5.42 (s, 2H), 4.60 (s, 2H). ^{13}C NMR (100 MHz, $CDCl_3$) δ: 164.12, 152.02, 144.36, 141.70, 134.58, 133.27, 133.12, 131.10, 129.86, 127.13, 124.41, 124.13, 122.98, 118.41, 110.04, 52.86, 26.75. LC-MS (ESI+APCI): *m/z* = 391 $[M + H]^+$.

2-(((1-(4-(Trifluoromethyl)benzyl)-1*H*-1,2,3-triazol-4-yl)methyl)thio)benzo[*d*]oxazole (BOT-16): Yield: 77%; off-white solid; m.p.: 81-83 ºC; IR (KBr, ν_{max}, cm^{-1}): 1504, 1322, 1112, 753; ^{1}H-NMR (400 MHz, $CDCl_3$) δ: 7.63 (s, 1H), 7.58-7.55 (m, 3H), 7.43-7.41 (m, 1H), 7.31-7.25 (m, 4H), 5.54 (s, 2H), 4.61 (s, 2H). ^{13}C NMR (100 MHz, $CDCl_3$) δ: 164.10, 152.02, 144.31, 141.71, 138.43, 131.45, 131.13, 128.10, 126.09, 126.05, 124.39, 124.14, 123.08, 118.39, 110.03, 53.46, 26.76. LC-MS (ESI+APCI): *m/z* = 391 $[M + H]^+$.

2-((4-((Benzo[*d*]oxazol-2-ylthio)methyl)-1*H*-1,2,3-triazol-1-yl)methyl)benzonitrile (BOT-17): Yield: 65%; off-white solid; m.p.: 74-76 ºC; IR (KBr, ν_{max}, cm^{-1}): 2227, 1498, 1217, 1136, 739; ^{1}H NMR (400 MHz, $CDCl_3$) δ: 7.88 (s, 1H), 7.68-7.66 (m, 1H), 7.61-7.59 (m, 1H), 7.55-7.51 (m, 1H), 7.45-7.41 (m, 2H), 7.31-7.22 (m, 3H), 5.70 (s, 2H), 4.62 (s, 2H). ^{13}C NMR (100 MHz, $CDCl_3$) δ: 163.55, 151.51, 143.68, 141.23, 137.48, 133.19, 132.59, 128.93, 128.85, 123.89, 123.59, 123.14, 118.02, 116.45, 111.26, 109.51, 51.25, 26.21. LC-MS (ESI+APCI): *m/z* = 348 $[M+H]^+$.

4-((4-((Benzo[*d*]oxazol-2-ylthio)methyl)-1*H*-1,2,3-triazol-1-yl)methyl)benzonitrile (BOT-18): Yield: 75%; off-white solid; m.p.: 70-72 ºC; IR (KBr, ν_{max}, cm^{-1}): 2228, 1503, 1227, 1131, 753; ^{1}H NMR (400 MHz, $CDCl_3$) δ: 7.69 (s, 1H), 7.58-7.54 (m, 3H), 7.43-7.41 (m, 1H), 7.31-7.25 (m, 4H), 5.54 (s, 2H), 4.60 (s, 2H). ^{13}C NMR (100 MHz, $CDCl_3$) δ: 164.03, 152.00, 144.47, 141.65, 139.65, 132.83, 128.30, 124.45, 124.22, 123.26, 118.38, 118.12, 112.71, 110.07, 53.39, 26.6. LC-MS (ESI+APCI): *m/z* = 348 $[M+H]^+$.

Methyl 4-((4-((benzo[*d*]oxazol-2-ylthio)methyl)-1*H*-1,2,3-triazol-1-yl)methyl)benzoate (BOT-19): Yield: 75%; off-white solid; m.p.: 75-77 ºC; IR (KBr, ν_{max}, cm^{-1}): 1722, 1502, 1281, 1131, 746; ^{1}H NMR (400 MHz, $CDCl_3$) δ: 7.98 (d, *J* = 8.4 Hz, 2H), 7.62 (s, 1H), 7.57-7.55 (m, 1H), 7.43-7.41 (m, 1H), 7.30-7.22 (m, 4H), 5.53 (s, 2H), 4.61 (s, 2H), 3.91 (s, 3H). ^{13}C NMR (100 MHz, $CDCl_3$) δ: 166.34, 164.10, 151.99, 144.16, 141.70, 139.34, 130.49, 130.31, 127.71, 124.36, 124.09, 123.10, 118.40, 110.01, 53.65, 52.27, 26.79. LC-MS (ESI+APCI): *m/z* = 381 $[M+H]^+$.

Docking studies: Docking studies were used to identify the conformation and special orientation at the active site of the target protein of synthesized molecules using GLIDE v3 (Schrodinger, Inc.) [25,26]. The extra precision method was a well-validated method which was used to generate the correct poses of ligands in the binding pocket of COX-2. Optimization was done to eliminate the unwanted conformations even though a comprehensive systematic exploration was performed. Monte Carlo sampling confirmed the pose by refining the generated

conformations. PDB ID-5KIR [27] was the crystal structure used for the studies and a human homology model of COX-1, which was generated and used in the absence of its crystal structure to explicate the selectivity issues. The initial crystal complex structure collected from protein data bank had concerns with hydrogen atoms, water molecules, tautomeric and protonation states of amino acids and hydroxyl group orientations and was refined.

The OPLS2005 force field was used to optimize and minimize the target. 15 Å, 15 Å, 15 Å box was defined on the centroid of the ligand present in the crystal structure to restrict the docking space. Care was taken to cover all the important amino acids within the centroid. Defaults were considered for all the remaining settings. Using the above settings all the synthesized molecules were docked into active site of COX-2. Since COX-1 homology model is well defined and validated, no further refinement was performed and used directly for docking. Human homology model of COX-1 was developed to study the selectivity of the synthesized molecules with COX-2. The amino acid sequence in FASTA format of human COX-1 was regained from Uniprot (A0S183_HUMAN).PSI (Protein Specific Iterated) BLAST algorithm [28] was used to categorize the similar protein structure (1EQG- a model of bovine COX-1 complexed with ibuprofen) [29] and were finalized based on the similarity percentage of the sequence.

Molecular dynamic simulations: Ligand receptor complex stability in a tangible environment was tested using molecular dynamic study. Predefined water model TIP4P was used to simulate with OPLS 2005 force field. To stipulate the size and shape of the unit an orthorhombic boundary was setup. The system was neutralized electrically by adding Na^+ ions arbitrarily. Desmond molecular dynamic simulation module with the periodic border circumstances in the NPT ensemble was used to minimize and relax the protein-ligand complex. Pressure and temperature were respectively fixed at 1 atmosphere and 300K using isotropic scaling and Nose-Hoover temperature coupling for running 100 ns NPT production simulation[30,31]. Configure rations were saved at 5 ps intermissions with a time step of 4.8 ps.

***in vitro* and *in vivo* Studies:** All the experiments of *in vitro* and *in vivo* studies were performed based on our previous published protocols [20,21].

RESULTS AND DISCUSSION

Molecular modelling studies: 2-Mercapto benzoxazole coupled benzyl triazoles (BOT) studies were carried out using standard Glide docking protocols. The structural analysis of the binding site of COX-2 revealed that a large hydrophobic cavity (LHC) was available at deep inside of binding pocket of COX-2, surrounded with hydrophobic and aromatic amino acids Val116, Val349, Leu352, Tyr355, Leu359, Val523, Ala527, Leu531 and Ser530. The deeper part of this pocket is occupied by the aromatic amino acids Phe381, Tyr385, Trp387 and Phe518 (Fig. 2).

In COX-1 binding pocket at this region, all the amino acids are conserved except Val523 and Arg513 present in COX-2 whereas Ile3 and His513 are present in COX-1. Because of

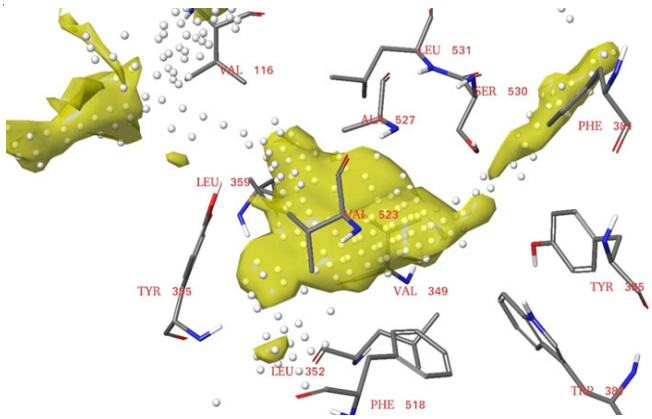

Fig. 2. Yellow contour represents the hydrophobic pocket of COX-2 Binding site with all important amino acids in designing the BOT analogues

the variations of amino acids, there is a deviation in the shape and increase in the size of the hydrophobic pocket occupying at this position which enhances the isoform selectivity [32,33]. In our previous work, 2-mercapto benzoxazole, which is obtained from scaffold hopping was proved to be active against COX-2.

The reported Aryl-triazolyl group against COX-2 [23] was coupled to generate the library of 2-mercapto benzoxazole coupled benzyl triazoles. Based on the structural analysis of LHC, we explored the aryl region of 2-mercapto benzoxazole aryl triazoles (BOT) by substituting the bulky groups to attain higher activity and selectivity for COX-2. Nineteen BOT analogues were designed and docked into the crystal structure of COX-2 to understand the hydrophobic interactions and binding energy.

Using the crystal coordinates of COX-2 co-crystallized with Vioxx ligand. That obtained from the protein data bank (PDB:5KIR), all the BOT analogues were docked in cyclooxygenase channel in place of Vioxx binding, using Glide XP tool. The docking studies generated stretched conformation of BOTs in the channel. The substituted aryl group occupying the deeper hydrophobic pocket has exposed the benzoxazole into solvent region (Fig. 3).

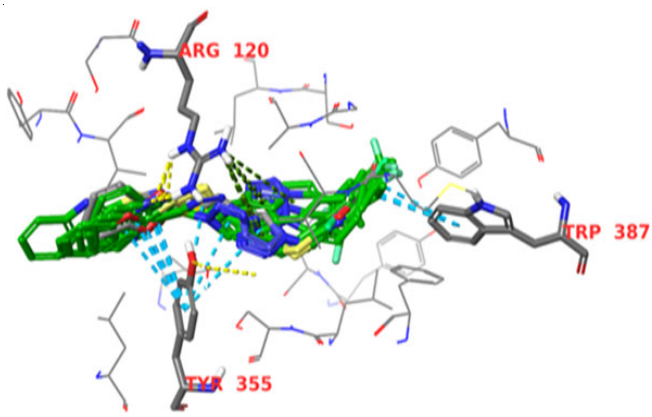

Fig. 3. Overlay of 19 analogues of BOT binding poses obtained from the docking inside the binding pocket of COX-2. Representation of hydrogen bond (yellow), stacking (sky blue), stacking (cation-phi) interactions with binding site amino acids

The docking score and binding energy using MMGBSA were calculated for all the compounds. The binding affinity between the inhibitors and the protein are highly dominated by the hydrophobic interactions. Benzoxazole moiety of the compounds is occupying the entrance of cyclooxygenase channel and forming a T-Shaped phi-phi stacking interaction with the phenyl ring of Tyr355. The most electronegative atom of benzoxazole ring, the nitrogen atom is forming a hydrogen bond with the guanidine group of Arg120. The cation nitrogen of Arg120 also forming cation-pi interactions with triazole ring. Substituted benzyl group attached to the triazole is occupied the LHC and forming strong dispersion interactions with nearby hydrophobic amino acids. Thus the hydrophobic substitutions accommodating in the pocket were showing high binding energy.

Compounds BOT-11, BOT-12, BOT-13, BOT-15 and BOT-19 having hydrophobic groups occupied at this position were having higher docking score than BOT-14, BOT-16 and BOT-18. In the case of BOT-15 and BOT-17, both have naphthalene ring at this position, BOT-15 has naphthalen-1-yl and was well oriented in the hydrophobic cavity (Fig. 4). But BOT-17 has naphthalen-2-yl and it has moved out of the pocket and had a steric clash with nearby amino acids. This might be the reason BOT-17 had reverse pose obtained during the docking calculations. The compounds with hydrophilic substituents (BOT-18, BOT-14) at this position were having relatively less binding energy than the hydrophobic substituents. To understand the binding interactions with the COX-1 protein, BOT analogues were docked and analyzed the results.

Almost all the interactions were conserved in COX-1 also, however, due to the small deviation of the LHC due to presence of Ile523, there was a small deviation of the pose orientation, the triazole ring losses it's Cation-Phi interaction with Arg120. This results in a small increase in the selectivity towards COX-2 over COX-1. A library of 2-mercapto benzoxazole coupled benzyl triazoles (BOT 1-19) were synthesized by copper acetate mediated click chemistry approach represented in **Scheme-I**.

2-(Prop-2-yn-1-ylthio)benzo[*d*]oxazole (**2**) was chosen as a key intermediate for the present study. Alkylation of benzo[*d*]oxazole-2-thiol (**1**) with propargyl bromide using K_2CO_3 as a base and DMF as a solvent at room temperature for 1 h to obtain 2-(prop-2-yn-1-ylthio)benzo[*d*]oxazole (**2**) in a magnificent yield. 2-(Prop-2-yn-1-ylthio)benzo[*d*]oxazole (**2**) was the key intermediate for the synthesis of triazoles derivatives (**BOT 1-19**). 2-(Prop-2-yn-1-ylthio)benzo[*d*]oxazole (**2**) was dissolved in EtOH/H_2O and then treated with different substi-

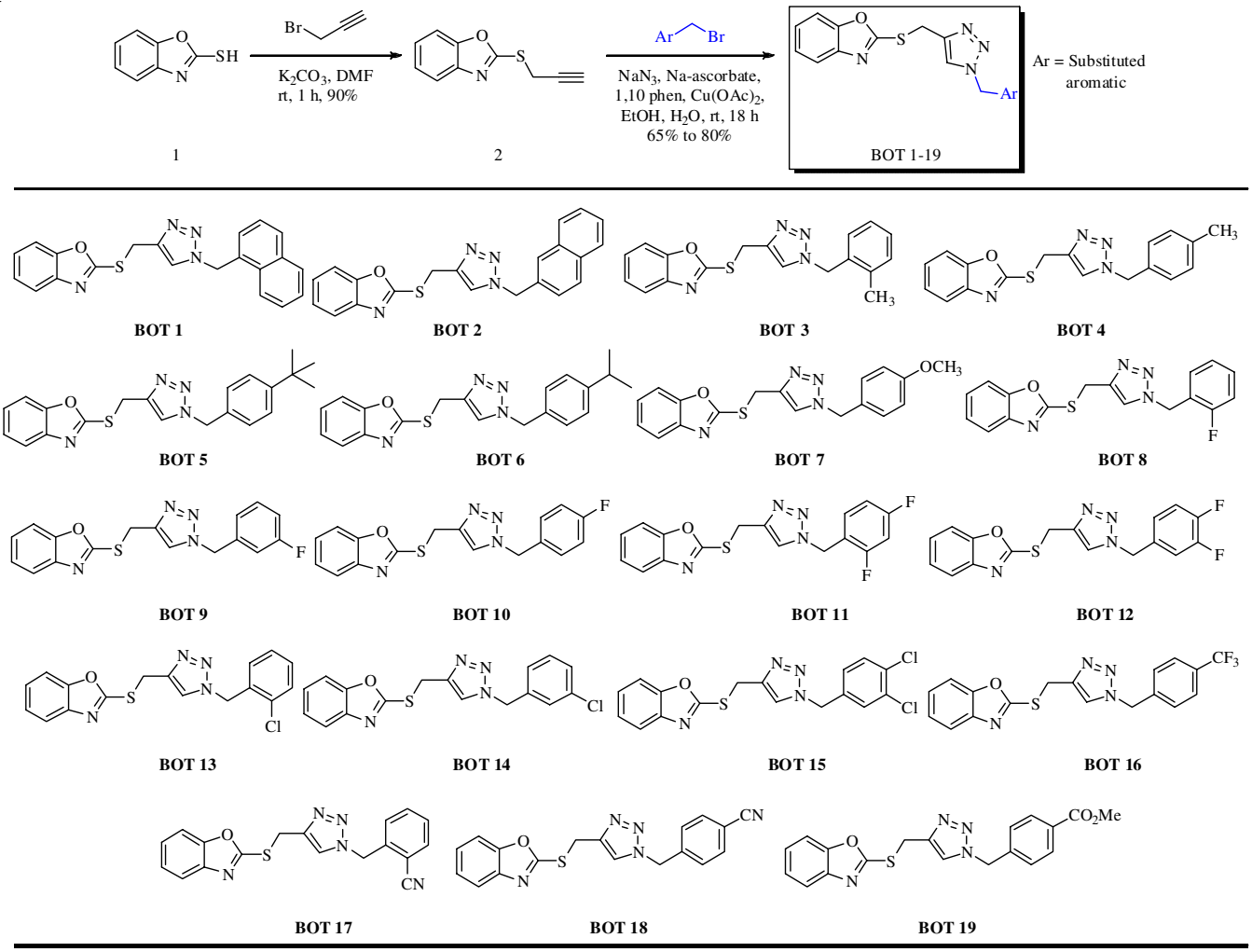

Scheme-I: Synthesis of 2-mercapto benzoxazole coupled with benzyl triazoles

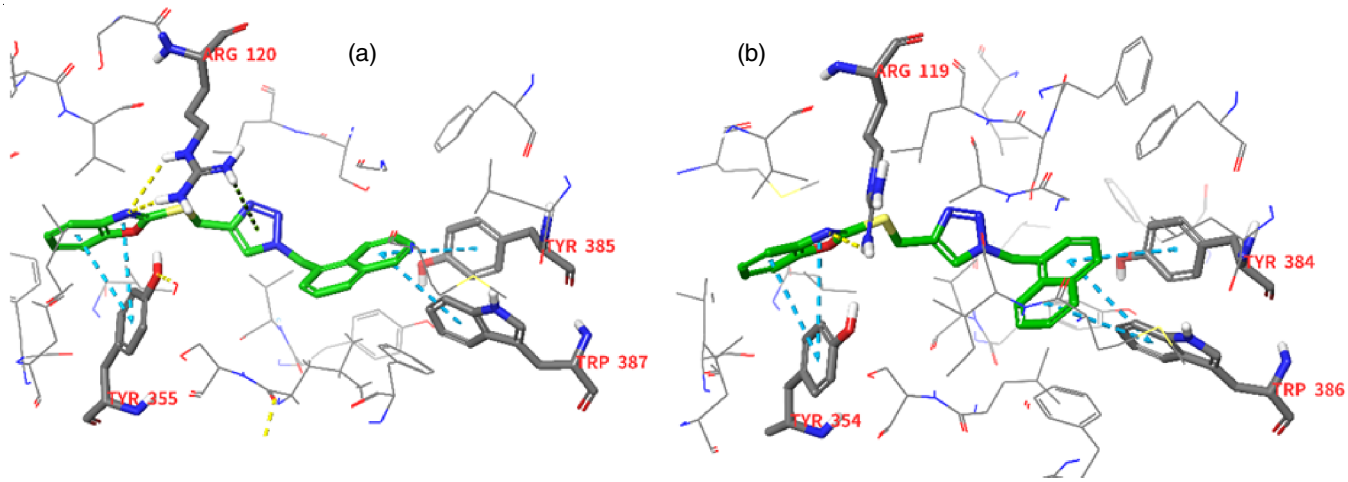

Fig. 4. Most active compound BOT 15 obtained from *in vitro* studies and its interactions with active site amino acids of COX-1 & COX-2

tuted benzyl bromides, followed with sodium ascorbate, catalytic amount of 1,10-phenanthroline monohydrate and $Cu(OAc)_2$ to obtain 2-mercapto benzoxazole coupled benzyl triazoles (**BOT 1-19**) in a moderate to good yields. There were minute changes were observed in the yields when compound **2** was treated with benzyl bromides bearing electron-donating groups (methyl, isopropyl, *tert*-butyl, methoxy) and electron-deficient groups (fluoro, chloro, cyano, trifluoromethyl, methyl ester).

Biological evaluation: BOT analogues (**BOT 1-19**) were tested for activity against COX enzymes for the activity and selectivity, followed by using *in vivo* anti-inflammatory activity assay to demonstrate the anti-inflammatory activity against animal models.

***in vitro* Anti-inammatory activity:** *in vitro* COX enzyme activity was measured using the standard protocol described by Copeland *et al*. [34]. The BOT analogues were initially evaluated at 10 µM drug concentrations and the per cent inhibitions were recorded. Indomethacin (COX-1 inhibitor) and celecoxib (selective COX-2 inhibitor) were used as positive controls in the study. All the compounds were showing greater than 50% inhibition against COX-2 except BOT-3, 4, 5, 11, 18 (Table-1). Compounds **BOT-6** and **14** showed 70% inhibitory activity at 10 µM concentrations. Compound **BOT-5** had a very low per cent activity (20% at 10 µM) among all the compounds. Almost two-fold selectivity was observed for the compounds **BOT-12** and **BOT-2**, however, the selectivity of the BOT analogues was much lower than the celecoxib (Fig. 5).

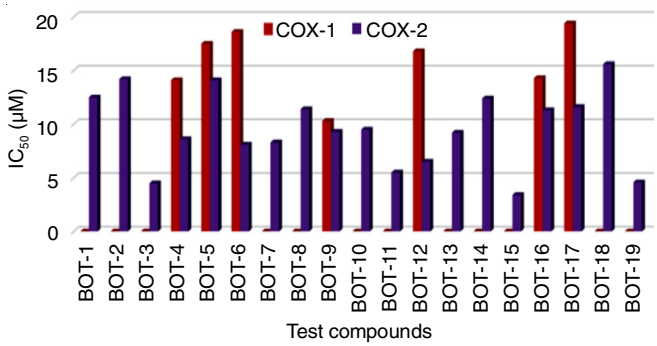

Fig. 5. *in vitro* Activity of all 19 BOTs against COX-1 & COX-2

TABLE-1
in vitro ANTI-INFLAMMATORY ACTIVITY OF BOTs

Compounds	Percentage of COX inhibition at 50 µM		COX inhibition (IC_{50} µM)	
	COX-1	COX-2	COX-1	COX-2
BOT-1	34.20	51.92	–	12.5
BOT-2	21.40	53.80	–	14.2
BOT-3	36.53	33.23	–	4.5
BOT-4	36.89	41.12	14.1	8.6
BOT-5	63.23	28.17	17.5	14.1
BOT-6	43.76	69.96	18.6	8.1
BOT-7	59.02	52.66	–	8.3
BOT-8	51.12	55.63	–	11.4
BOT-9	51.44	66.28	10.3	9.3
BOT-10	43.86	63.86	–	9.5
BOT-11	35.54	47.67	–	5.5
BOT-12	37.21	65.01	16.8	6.5
BOT-13	48.54	55.01	–	9.2
BOT-14	65.51	71.07	–	12.4
BOT-15	38.85	51.59	–	3.4
BOT-16	43.47	57.24	14.3	11.3
BOT-17	50.62	51.67	19.4	11.6
BOT-18	44.46	40.51	–	15.6
BOT-19	48.63	52.51	–	4.57
Indomethacin	65.40	23.20	NT	NT
Celecoxib	15.10	93.40	NT	0.36

Further, IC_{50} values were determined for COX-1 and COX-2 to understand the precise inhibitory activity of the compounds. Significantly, all the compounds showed IC_{50} (half maximal inhibitory concentration) close to 10 µM against COX-2. The IC_{50} values of these compounds and the *in-silico* binding energies that is Glide score and the MMGBSA had a reasonable correlation (r^2) of 0.62 and 0.63, respectively (Fig. 6).

The highest active compounds had less than -8.2 Kcal/mol Glide score and less than -40 Kcal/mol MMGBSA energy. This benchmarking helped to use the criteria as a filter for our future selection of design. Among all the compounds, **BOT-15** showed highest IC_{50} of 3.4 µM followed by **BOT-19** (4.5 µM), **BOT-3** (4.5 µM), **BOT-11** (5.5 µM) and **BOT-12** (6.5 µM).

As discussed in the docking studies, the compounds, which had hydrophobic group substituted on the aryl group, formed strong hydrophobic interactions with the LHC amino acids.

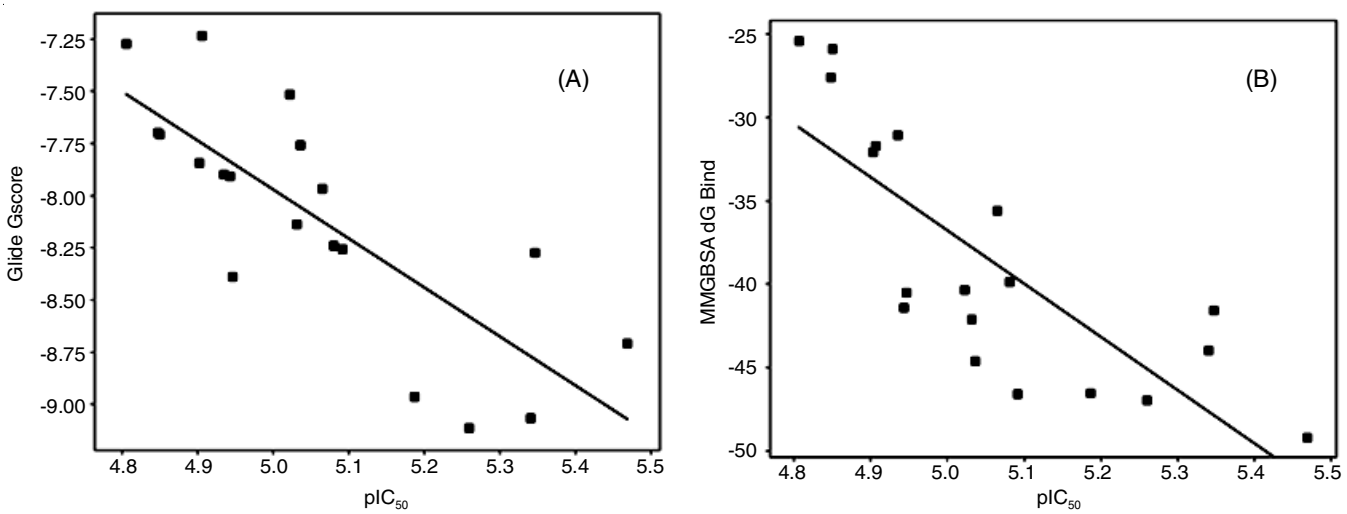

Fig. 6. Correlation graphs A. Correlation between experimental pIC_{50} and Glide score, B. Correlation between pIC_{50} and MMGBSA

Further, the stability of **BOT-15** inside the pocket of COX-2 was determined by running the molecular dynamic simulation for with 100 ns time in solvent water (TIP4P). The protein was stable throughout the dynamics and has the RMSD near 2.0 Å. The ligand was also reasonably stable and had RMSD in the range of 1 to 2 Å (Fig. 7).

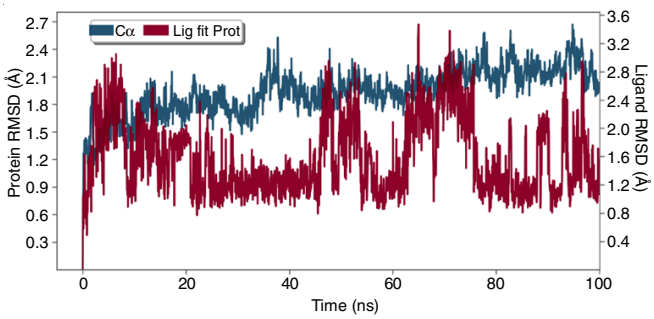

Fig. 7. RMSD of all the frames of the trajectory obtained from the 100ns Molecular dynamic simulations

The average protein-ligand contacts throughout the dynamics (Fig. 8) showed that the interaction between the guanidine of Arg120 and nitrogen of benzoxazole conversed throughout the dynamics. Additional interaction was observed in the dynamics with side-chain OH formed hydrogen bond with the triazole nitrogen atom. From the molecular docking studies, it was understood that naphthalene-2-yl of BOT-18 had steric hinderances with the receptor amino. BOT analogues exhibited IC_{50} near to 10 µM even for the COX-1 enzyme also and hence they had very less selectivity over COX-1. The withdrawn drug, celecoxib has very good activity and high selectivity, sulphonamide moiety of celecoxib designed to bind within the side pocket to provide isoform-selective inhibition [35] which is formed by Arg513 of COX-2, absent in COX-1. The selectivity of the BOT can be improved by designing the analogues to interact with the amino acids of the side pocket.

***in vivo* Anti-inflammatory studies:** Out of nineteen BOTs, nine most active BOT analogues obtained after their *in vitro* studies were further evaluated for *in vivo* efficacy and compared

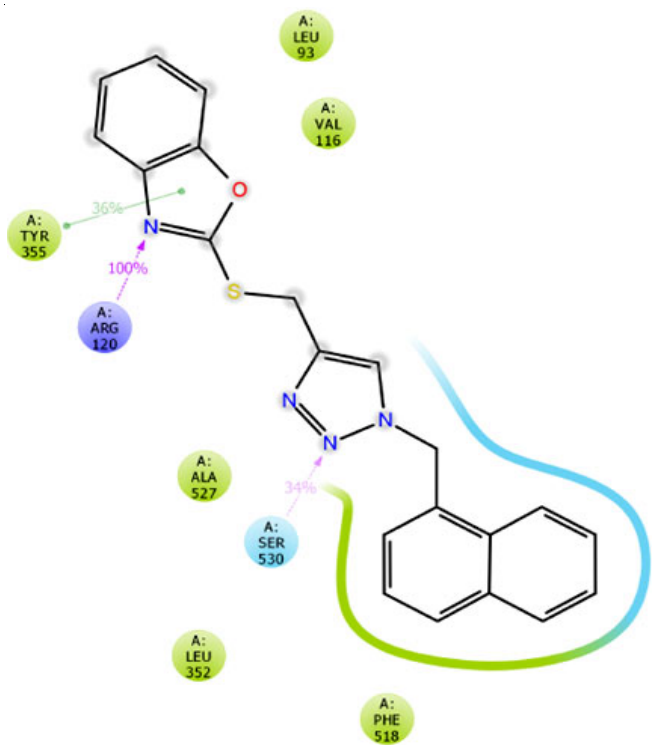

Fig. 8. A schematic diagram of the overall percentage interactions of BOT-15 with the protein residues obtained after 100 ns molecular dynamic simulations

with the standard drug ibuprofen. The *in vivo* studies were evaluated by carrageen induced paw edema analysis according to the previously reported method [36]. The anti-inflammatory activity of nine BOTs was carefully analyzed after oral administration of amount 10mg/kg/body weight. The results were very encouraging, **BOT-12** and **BOT-13** showed more than 70% inhibition of the inflammation in 3 h (Table-2). Especially, compound **BOT-13** had a higher percentage of inhibition than ibuprofen. Interestingly, the most active compound **BOT-15**, obtained in *in vitro* studies had lesser inhibition than these compounds which may be attributed to permeability issues. All the compounds have very good inhibition at 5 h on comp-

TABLE-2
ACTIVITY OF BOTs EVALUATED *in vivo* FOR THE CHANGE IN PAW EDEMA VOLUME (mL) AFTER DRUG TREATMENT AND ANTI-INFLAMMATORY ACTIVITY % OF INHIBITION

Compounds	Change in Paw edema volume (mL) after drug treatment		Anti-inflammatory activity % of inhibition	
	3 h	5 h	3 h	5 h
Control	0.86 ± 0.173	0.87 ± 0.140	–	–
BOT-3	0.11 ± 0.051	0.10 ± 0.051	60.62	84.94
BOT-4	0.31 ± 0.038	0.22 ± 0.157	62.71	62.56
BOT-6	0.27 ± 0.045	0.24 ± 0.122	61.24	65.93
BOT-7	0.28 ± 0.069	0.18 ± 0.040	67.44	68.31
BOT-11	0.28 ± 0.078	0.26 ± 0.086	60.62	61.23
BOT-12	0.22 ± 0.550	0.26 ± 0.205	70.97	69.76
BOT-13	0.35 ± 0.035	0.39 ± 0.050	75.04	85.56
BOT-15	0.27 ± 0.069	0.38 ± 0.040	66.44	56.38
BOT-19	0.17 ± 0.078	0.16 ± 0.086	60.62	61.24
Ibuprofen	0.24 ± 0.135	0.34 ± 0.145	72.48	61.30

arison with ibuprofen except compound **BOT-15** (Fig. 9). Compounds **BOT-3** and **BOT-13** had excellent inhibition of 85% for 5 h and these two compounds could be further developed into drug candidates after improving the selectivity.

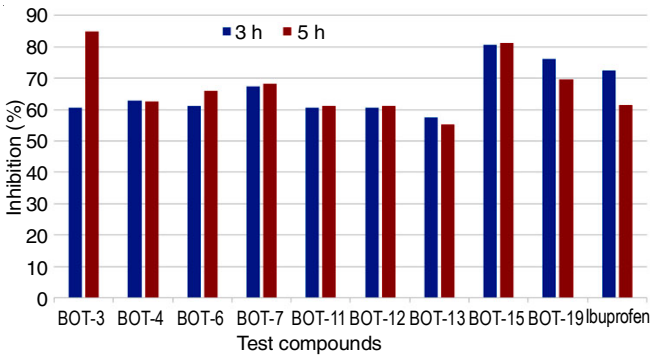

Fig. 9. *in vivo* Anti-inflammatory effect of BOTs

Antioxidant activity: Antioxidant activity of all the BOTs was performed using 2,2-diphenyl-1-picrylhydrazyl (DPPH) radical scavenging assay. Molecules at diverse estimates were prepared and verified their activity using DPPH free radicals. Ascorbic acid was used as a standard. Inhibition concentration (IC_{50}) of all the BOTs synthesized were active and proved efficient than the standard used. All the BOTs can neutralize the reactive oxygen species efficiently when compared with ascorbic acid. Compounds **BOT8**, **BOT10** and **BOT19** having IC_{50} values of 8.62, 10.67 and 11.56 µM, respectively were the most active antioxidants among all the tested compounds (Fig. 10). Compounds **BOT5**, **BOT6** and **BOT18** displayed a similar type of activity (19.04, 18.14 and 18.60 µM) as ascorbic acid (20.70 µM). The character of BOTs in altering the free radicals into neutral or less reactive species was good and hence proved to be potent and effective free radical scavengers.

Conclusion

In this work, nineteen 2-mercapto benzoxazole coupled benzyl triazoles (BOTs) analogues were designed, synthesized and validated using *in vitro* and *in vivo* studies to identify the potential COX-2 inhibitors. The most potent among the BOT analogues were **BOT15**, **BOT3** and **BOT19** with IC_{50} 3.4, 4.50 and 4.57 µM, respectively against COX-2. The *in vivo* studies

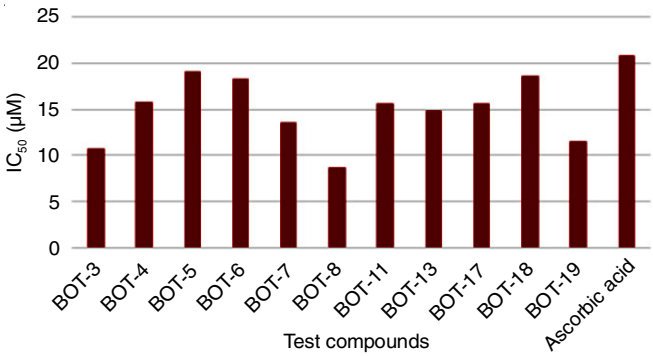

Fig. 10. Antioxidant activity (IC_{50}) of BOTs in µM

showed two compounds **BOT3** and **BOT15** have more than 80% anti-inflammatory activity at 5 h, which is more efficient than the standard COX-2 drug.

ACKNOWLEDGEMENTS

One of the authors, K.P., thanks the Council of Scientific and Industrial Research (CSIR), New Delhi, India for financial assistance in the form of research fellowships. Another author, J.S.Y. Former Director, IICT, Hyderabad, India thanks CSIR, New Delhi for the award of Bhatnagar Fellowship.

CONFLICT OF INTEREST

The authors declare that there is no conflict of interests regarding the publication of this article.

REFERENCES

1. D.H. Tsai, D.H. Amyai, N. Marques-Vidal, P. Wang, J.L. Riediker, M. Mooser, V. Paccaud, F. Waeber, G. Vollenweider and M. Bochud, *Part. Fibre Toxicol.*, **9**, 24 (2012); https://doi.org/10.1186/1743-8977-9-24
2. E.D. Högestätt, B.A.G. Jönsson, A. Ermund, D.A. Andersson, H. Björk, J.P. Alexander, B.F. Cravatt, A.I. Basbaum and P.M. Zygmunt, *J. Biol. Chem.*, **280**, 31405 (2005); https://doi.org/10.1074/jbc.M501489200
3. J.L. Wallace, *Physiol. Rev.*, **88**, 1547 (2008); https://doi.org/10.1152/physrev.00004.2008
4. S.X. Sun, K.Y. Lee, C.T. Bertram and J.L. Goldstein, *Curr. Med. Res. Opin.*, **23**, 1859 (2007); https://doi.org/10.1185/030079907X210561

5. M.D. Ferrer, C. Busquets-Cortés, X. Capó, S. Tejada, J.A. Tur, A. Pons and A. Sureda, *Curr. Med. Chem.*, **26**, 3225 (2019); https://doi.org/10.2174/0929867325666180514112124
6. M.J. Alam, O. Alam, S.A. Khan, M.J. Naim, M. Islamuddin and G.S. Deora, *Drug Des. Devel. Ther.*, **10**, 3529 (2016); https://doi.org/10.2147/DDDT.S118297
7. S.Z. Ren, Z.C. Wang, X.H. Zhu, D. Zhu, Z. Li, F.Q. Shen, Y.T. Duan, H. Cao, J. Zhao and H.L. Zhu, *Bioorg. Med. Chem. Lett.*, **26**, 4264 (2018); https://doi.org/10.1016/j.bmc.2018.07.022
8. P.F. Lamie, W.A.M. Ali, V. Bazgier and L. Rárová, *Eur. J. Med. Chem.*, **123**, 803 (2016); https://doi.org/10.1016/j.ejmech.2016.08.013
9. P. Singh, P. Prasher, P. Dhillon and R. Bhatti, *Eur. J. Med. Chem.*, **97**, 104 (2015); https://doi.org/10.1016/j.ejmech.2015.04.044
10. Y.K. Márquez-Flores, M.E. Campos-Aldrete, H. Salgado-Zamora, J. Correa-Basurto and M.E. Meléndez-Camargo, *Med. Chem. Res.*, **21**, 3491 (2012); https://doi.org/10.1007/s00044-011-9870-3
11. M. Ahmed, M.A. Qadir, A. Hameed, M. Imran and M. Muddassar, *Chem. Biol. Drug Des.*, **91**, 338 (2018); https://doi.org/10.1111/cbdd.13076
12. L.W. Mohamed, O.M. El-Badry, A.K. El-Ansary and A. Ismael, *Bioorg. Chem.*, **72**, 308 (2017); https://doi.org/10.1016/j.bioorg.2017.04.012
13. A.K. Shakya, A. Kaur, B.O. Al-Najjar and R.R. Naik, *J. Saudi Pharm.*, **24**, 616 (2016); https://doi.org/10.1016/j.jsps.2015.03.018
14. C. Battilocchio, G. Poce, S. Alfonso, G.C. Porretta, S. Consalvi, L. Sautebin, S. Pace, A. Rossi, C. Ghelardini, L.D. Mannelli, S. Schenone, A. Giordani, L. Di Francesco, P. Patrignani and M. Biava, *Bioorg. Med. Chem.*, **21**, 3695 (2013); https://doi.org/10.1016/j.bmc.2013.04.031
15. K.J. Kim, M.J. Choi, J.S. Shin, M. Kim, H.E. Choi, S.M. Kang, J.H. Jin, K.T. Lee and J.Y. Lee, *Bioorg. Med. Chem. Lett.*, **24**, 1958 (2014); https://doi.org/10.1016/j.bmcl.2014.02.074
16. E.S. Taher, T.S. Ibrahim, M. Fares, A.M.M. AL-Mahmoudy, A.F. Radwan, K.Y. Orabi and O.I. El-Sabbagh, *Eur. J. Med. Chem.*, **171**, 372 (2019); https://doi.org/10.1016/j.ejmech.2019.03.042
17. E.M. Ahmed, A.E. Kassab, A.A. El-Malah and M.S.A. Hassan, *Eur. J. Med. Chem.*, **171**, 25 (2019); https://doi.org/10.1016/j.ejmech.2019.03.036
18. J. Elie, J. Vercouillie, N. Arlicot, L. Lemaire, R. Bidault, S. Bodard, C. Hosselet, J.B. Deloye, S. Chalon, P. Emond, D. Guilloteau, F. Buron and S. Routier, *J. Enzyme Inhib. Med. Chem.*, **34**, 1 (2019); https://doi.org/10.1080/14756366.2018.1501043
19. M. Murahari, V. Mahajan, S. Neeladri, M.S. Kumar and Y.C. Mayur, *Bioorg. Chem.*, **86**, 583 (2019); https://doi.org/10.1016/j.bioorg.2019.02.031
20. S. Yatam, S.S. Jadav, R. Gundla, K.P. Gundla, G.M. Reddy, M.J. Ahsan and J. Chimakurthy, *ChemistrySelect*, **3**, 10305 (2018); https://doi.org/10.1002/slct.201801558
21. S. Yatam, R. Gundla, S.S. Jadav, N. Pedavenkatagari, J. Chimakurthy, N. Rani B and T. Kedam, *J. Mol. Struct.*, **1159**, 193 (2018); https://doi.org/10.1016/j.molstruc.2018.01.060
22. R. Paramashivappa, P. Phani Kumar, P.V. Subba Rao and A. Srinivasa Rao, *Bioorg. Med. Chem. Lett.*, **13**, 657 (2003); https://doi.org/10.1016/S0960-894X(02)01006-5
23. S. Shafi, M. Mahboob Alam, N. Mulakayala, C. Mulakayala, G. Vanaja, A.M. Kalle, R. Pallu and M.S. Alam, *Eur. J. Med. Chem.*, **49**, 324 (2012); https://doi.org/10.1016/j.ejmech.2012.01.032
24. K. Seth, S.K. Garg, R. Kumar, P. Purohit, V.S. Meena, R. Goyal, U.C. Banerjee and A.K. Chakraborti, *Med. Chem. Lett.*, **5**, 512 (2014); https://doi.org/10.1021/ml400500e
25. R.A. Friesner, R.B. Murphy, M.P. Repasky, L.L. Frye, J.R. Greenwood, T.A. Halgren, P.C. Sanschagrin and D.T. Mainz, *J. Med. Chem.*, **49**, 6177 (2006); https://doi.org/10.1021/jm051256o
26. T.A. Halgren, R.B. Murphy, R.A. Friesner, H.S. Beard, L.L. Frye, W.T. Pollard and J.L. Banks, *J. Med. Chem.*, **47**, 1750 (2004); https://doi.org/10.1021/jm030644s
27. B.J. Orlando and M.G. Malkowski, *Acta Crystallogr. F: Struct. Biol. Commun.*, **47**, 772 (2016); https://doi.org/10.1107/S2053230X16014230
28. S.F. Altschul, W. Gish, W. Miller, E.W. Myers and D.J. Lipman, *J. Mol. Biol.*, **215**, 403 (1990); https://doi.org/10.1016/S0022-2836(05)80360-2
29. B.S. Selinsky, K. Gupta, C.T. Sharkey and P.J. Loll, *Biochemistry*, **40**, 5172 (2001); https://doi.org/10.1021/bi010045s
30. Y. Shan, M.A. Seeliger, M.P. Eastwood, F. Frank, H. Xu, M.O. Jensen, R.O. Dror, J. Kuriyan and D.E. Shaw, *Proc. Natl. Acad. Sci. USA*, **106**, 139 (2009); https://doi.org/10.1073/pnas.0811223106
31. K.K. Raj, V.G. Kumar, C.L. Madhuri, P. Mathi, R.D. Lakshmi, M. Ravi, B.S. Ramudu, S.V. Venkata Rao and D. Ramachandran, *J. Mol. Graph. Model.*, **60**, 89 (2015); https://doi.org/10.1016/j.jmgm.2015.05.009
32. E. Wong, C. Bayly, H.L. Waterman, D. Riendeau and J.A. Mancini, *J. Biol. Chem.*, **272**, 9280 (1997); https://doi.org/10.1074/jbc.272.14.9280
33. J.K. Gierse, J.J. McDonald, S.D. Hauser, S.H. Rangwala, C.M. Koboldt and K.J. Seibert, *Biol. Chem.*, **271**, 15810 (1996); https://doi.org/10.1074/jbc.271.26.15810
34. R.A. Copeland, J.M. Williams, J. Giannaras, S. Nurnberg, M. Covington, D. Pinto, S. Pick and J.M. Trzaskos, *Proc. Natl. Acad. Sci. USA*, **91**, 11202 (1994); https://doi.org/10.1073/pnas.91.23.11202
35. L.J. Marnett, *Annu. Rev. Pharmacol. Toxicol.*, **49**, 265 (2009); https://doi.org/10.1146/annurev.pharmtox.011008.145638
36. C.A. Winter, E.A. Risley and G.W. Nuss, *Proc. Soc. Exp. Biol. Med.*, **111**, 544 (1962); https://doi.org/10.3181/00379727-111-27849